Journal of Materials Chemistry C

Accepted Manuscript

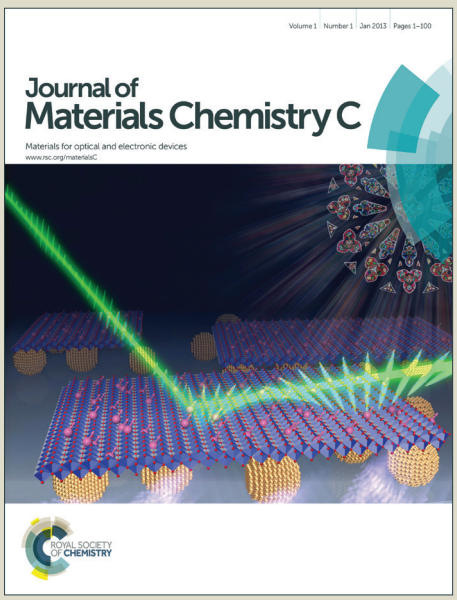

ROYAL SOCIETY OF CHEMISTRY

www.rsc.org/materialsC

Journal of Materials Chemistry C RSCPublishing

PAPER

Effects of Fluorination on the Electrochromic Performance of Benzothiadiazole-Based Donor-Acceptor Copolymers

Cite this: DOI: 10.1039/xoxxoooooox

Received ooth January 2014,
Accepted ooth January 2014

DOI: 10.1039/xoxxoooooox

www.rsc.org/

Wei Teng Neo,[a,b,†] Kok Haw Ong,[a,†] Ting Ting Lin,[a] Soo-Jin Chua,[a,c] and Jianwei Xu[a,d,*]

A series of thiophene and benzothiadiazole-based copolymers (**PDAT-DTBT**) is synthesized through Stille coupling polymerization with two mono- and di-fluorinated benzothiadiazole analogues: **PDAT-DTBT-F** (1F) and **PDAT-DTBT-2F** (2F). The introduction of fluorine atoms onto the conjugated polymer backbone is found to have a pronounced effect on the optical, electrochemical and morphological properties, which in turn, influences the electrochromic performance of the fabricated absorption/transmission type devices greatly. All the polymers switch reversibly between the colored neutral states (green/blue) to transmissive oxidized states. Systematic enhancement in the reduction process to sub-second speeds (<0.5 s), high coloration efficiency (748 cm^2/C) and substantially improved ambient stability are observed upon fluorination of electron acceptors. Long-term stability testing of electrochromic device is carried out for **PDAT-DTBT-F** for up to 10, 000 repeated redox cycles between applied potentials of +1.6 and -1.6 V, without the observation of significant degradation.

Introduction

The field of electrochromic polymers has received widespread attention, and rapid advances have been realized in recent years.[1-10] Electrochromic polymers, displaying variable optical and transmittance changes upon application of an external bias, are potentially applicable in various technologies such as smart windows, electronic displays and camouflage cloths. Along with their ease of structural modifications for the tuning of physical and chemical properties, conjugated polymers are also flexible, light-weight and low-cost. These advantages make them ideal for use in optoelectronic devices.

The donor-acceptor (D–A) approach[11-13] has been a successful strategy to achieve low-bandgap polymers with tunable optical absorbance in the field of electrochromics. Among the numerous acceptor moieties that have been used in D–A polymers, 2,1,3-benzothiadiazole (BTD) has been intensively investigated and it has established itself as a promising building block for electrochromic polymers.[14-24] The BTD acceptor unit is commonly co-polymerized with electron-donating 3,4-dioxythiophene based moieties to yield excellent electrochromic materials with high optical contrasts and rapid switching speeds coupled with high coloration efficiencies.[24] More importantly, such materials exhibit extreme redox stabilities and hold the highest record for cycle life among reported polymers to-date.[17] Besides bandgap tuning, the presence of alternating electron-rich and electron-deficient units in a D–A type polymer can lead to strong intramolecular charge transfer between the two moieties. This greatly influences the energies of the frontier molecular orbitals which, in turn, determine the redox behavior of the polymers. Careful manipulation of the highest-occupied molecular orbital (HOMO) and lowest-occupied molecular orbital (LUMO) is thus required to achieve high-performing devices.

Recently, the incorporation of fluorine atoms onto the conjugated backbone has been observed to affect the HOMO and LUMO energy levels.[25] Using this strategy, considerable success has been yielded in enhancing the performance of various organic electronics such as improving the conversion efficiency of photovoltaic cells,[26-37] increasing the ambient stability of thin-film transistors,[38] as well as the color stability and electroluminescence properties of polymer-based light-emitting diodes.[39] In general, the performance improvements in organic electronics are attributed to the effective lowering of the HOMO and LUMO energy levels of the polymers and increasing intra- and inter-molecular interactions.[34] In this regard, fluorine is an excellent substituent due to its high electronegativity and small atomic radius, which allows the properties of the polymers to be manipulated without inducing undesirable steric hindrance.[37] To the best of our knowledge, the effect of fluorination of electron acceptors on the electrochromic performance of conjugated polymers has not been investigated. Hence, it is of significance to explore the electrochromic properties of the fluorinated polymers.

Herein we report the design and synthesis of BTD-based donor-acceptor copolymers with two fluorinated analogues, namely, **PDAT-DTBT** (0F), **PDAT-DTBT-F** (1F) and **PDAT-DTBT-2F** (2F). The role of the additional electron-withdrawing fluorine atoms on the physical, chemical, morphological, and resultant electrochromic properties of the polymers are fully investigated.

Results and discussion

Synthesis and characterization

The synthetic route for the polymers is shown in **Scheme 1**. Detailed synthesis steps are provided under the experimental section. 2,5-dibromo-3,4-bis(2-hexyldecyloxy)thiophene **2** was synthesized by reacting 3,4-dimethoxythiophene with 2-hexyldecanol using an etherification reaction,[40] followed by bromination with NBS with an overall yield of over 90%.[41] Fluorinated monomers **4b** and **4c** were synthesized using the method previously reported for the synthesis of 4,7-bis(2-trimethylstannylthien-5-yl)-2,1,3-benzothiadiazole **4a**.[42] The polymerizations were carried out at 120 °C in chlorobenzene using $Pd_2(dba)_3$ as the catalyst and P(*o*-tol)$_3$ as the ligand. The yields of the polymers were between 57 and 85%, and number-averaged molecular weights between 6.7 and 20.0 kg mol^{-1} were obtained (Table 1).

Thermal properties

Thermogravimetric analysis (TGA) and differential scanning calorimetry (DSC) were performed on the polymers. The polymers exhibited excellent thermal stability, with all the polymers having 5 % weight loss temperatures (T_d) of around 335 °C (Table 1). DSC scans revealed no significant phase transitions within the range of -20 to 300 °C (see supporting information).

Optical and electrochemical properties

The normalized UV-visible absorption spectra of **PDAT-DTBT**, **PDAT-DTBT-F** and **PDAT-DTBT-2F** in chlorobenzene solution and as thin films are shown in Fig. 1a. All the polymers exhibit two distinct absorption bands, characteristic of D–A type polymers. The higher energy band (~420 nm) can be attributed to the localized π-π* transition, whereas the broader, lower energy band (620-650 nm) is assigned to the intramolecular charge transfer (ICT) interaction between the donor and BTD-based acceptor units.[33] Going from the solution to thin film state, minimal changes are observed for **PDAT-DTBT.** On the other hand, there is a slight broadening and bathochromic shift in absorption onset of the low-energy band for the fluorinated polymers, which suggests further aggregation in the solid state. In addition, the lower energy band splits and results in the formation of a distinct vibronic shoulder, especially for **PDAT-DTBT-F** and **PDAT-DTBT-2F**, implying an increased π-π stacking of the polymer backbone and enhanced intermolecular interactions. Interestingly, the increasing addition of F atoms onto the polymer backbone leads to a systematic hypsochromic shift of the absorption maxima (λ_{max}) and absorption onset (λ_{onset}) from 652 to 648 to 625 nm and 800 to 782 to 772 nm respectively, which is consistent with previous observations.[27, 36, 37] The hypsochromic shifts of λ_{max} and λ_{onset} in fluorinated polymers may be attributable to the increased steric hindrance owing to the larger atomic radius of the fluorine atoms (compared to hydrogen), leading to a reduced effective conjugation length. Nonetheless, the interaction of the fluorine atoms with the neighbouring sulfur atoms encourages planarization of the polymer backbone and effectively limits the extent of steric twisting. As such, the blue-shifts are minimal.[30] With increasing backbone fluorination, the optical band gaps increase slightly with **PDAT-DTBT**, **PDAT-DTBT-F** and **PDAT-DTBT-2F** exhibiting band gaps of 1.55, 1.59 and 1.61 eV respectively.

The redox behaviour, as well as the HOMO and LUMO energy levels of the polymers was probed using cyclic voltammetry. Fig. 1b depicts the cyclic voltammograms of the polymer thin films. All three polymers reveal quasi-reversible oxidation and reduction properties. Based on the oxidation onset potentials, the HOMO energy levels were determined. It is observed that the HOMO levels are lowered systematically upon increasing addition of the electron-withdrawing F substituents (-5.22 → -5.24 → -5.31 eV), which is in agreement with previous reports.[27, 34, 36, 37, 43] With deeper HOMO energy levels, fluorinated polymers are envisaged to have improved ambient stability. The LUMO energy levels were approximated from the HOMO levels and the optical band gaps. All three polymers revealed similar LUMO levels in the range of -3.65 to -3.70 eV. The spectroscopic and electrochemical data are summarized in Table 2.

Computational calculations

To better understand the effect of fluorination on the minimum-energy conformation of the polymers, time-dependent density functional theory (TD-DFT) calculations at B3LYP/6-31G(d) theory level was carried out for the simplified dimeric model compounds of **PDAT-DTBT**, **PDAT-DTBT-F** and **PDAT-DTBT-2F** (Fig. 2). The branched alkoxy side chains are replaced with methoxy groups for simplicity. The HOMO and LUMO levels, as well as the dihedral angles of the optimized structures were also calculated (Table S1 and Fig. 2). In all three polymers, high molecular planarity is observed within the monomer which extends slightly into the dimer, which is in good agreement with previous report that the incorporation of fluorine atoms imparts negligible steric hindrance to the effective conjugation of the backbone.[37] From the molecular orbital distributions, it is shown that the HOMO is well-delocalized over the whole π-backbone for all three polymers. On the other hand, the LUMO is concentrated on the BTD-based acceptors. As illustrated in **PDAT-DTBT-2F**, the fluorine atoms are covered in both the HOMO and LUMO profiles, suggesting that the fluorine atoms are contributing both inductively and mesomerically through its electron-withdrawing nature and available lone pairs respectively.[43] Consistent with our experimental findings, DFT calculations revealed a systematic lowering of both HOMO and LUMO energy levels upon fluorination, with comparable energy gaps across all three polymers.

Electrochromic device performance

The electrochromic behavior of the polymers was studied in single-layer absorption/transmission type devices with a cell configuration of glass/ITO/polymer/gel electrolyte/ITO/glass. Details for the fabrication process are provided in the experimental section. The spectroelectrochemical spectra of the polymers are illustrated in Fig. 3. The UV-visible-NIR absorptions of the polymers are recorded upon progressive oxidation from their neutral states to 2.0 V. At their neutral states, **PDAT-DTBT**, **PDAT-DTBT-F** and **PDAT-DTBT-2F** reveal green, blue-green and blue hues respectively. With increasing applied potential, both the π-π* and ICT absorption peaks are depleted with a concomitant formation of the polaron and bipolaron bands in the NIR region. For all three polymers, the polaron absorption occurs at around 900 nm and peaks at approximately 1.6 V. Upon further oxidation, the polaronic bands start to drop in intensity while the bipolaronic band grows further. For **PDAT-DTBT** and **PDAT-DTBT-F**, the absorption corresponding to the polaron is completely depleted at 2.0 V whereas **PDAT-DTBT-2F** reveals residual absorption. This illustrates that electrochemical p-doping for **PDAT-DTBT-2F** is the most difficult to achieve, possibly due to its low-lying HOMO level. At their 2.0 V states, the polymers are strongly NIR-absorbing, with only slight tailing of the absorptions into the visible region. As such, all the polymers appear transmissive light grey (Fig. 3). Distinct isosbestic points (~750 and 1000 nm) are also observed for the three polymers, which confirm the presence of more than one interconverting species, possibly the neutral, polaronic and bipolaronic states.[44, 45]

To characterize the degree of absorption changes of the polymers in both the visible and NIR regions, a square-wave potential step absorptiometry was utilized. In-situ transmittance changes of the polymers were measured while they were being subjected to redox switching between +1.6 and -1.6 V. The optical contrasts are taken as the absolute difference in transmittance between the oxidized and reduced states, while switching times are calculated based on the time taken to reach 95 % of the full switch. The results are shown in Fig. 4 and summarized in Table 3. An asymmetry between bleaching and coloration response time is apparent and the effects of fluorination on the switching speeds are evident. Going from **PDAT-DTBT**, **PDAT-DTBT-F** to **PDAT-DTBT-2F**, the disparity is widened as the oxidation process is hindered whereas the reduction process is facilitated. In the visible region, the oxidation process corresponds to the bleaching of the polymer while the reduction process corresponds to the coloration. In the NIR region, the processes are reversed. For instance in the visible region, the bleaching speed (oxidation) is moderately reduced (32.7 → 53.2 → 62.4 s) upon successive incorporation of F atoms, whereas the coloration speed (reduction) is improved by more than a factor of 10 to subsecond switching (4.62 → 0.75 → 0.42 s). A similar trend is observed in the NIR region. The difference in the switching speeds may possibly be explained by the increased electron affinity of the fluorinated polymers, which leads to the polymers' reduced susceptibility towards electrochemical oxidation while, on the other hand, accepting electrons readily, as evident from the deeper HOMO and LUMO energy levels. Despite the differences in switching speeds, **PDAT-DTBT** and **PDAT-DTBT-F** exhibit comparable optical contrasts in both the visible and NIR regions at approximately 30 and 55 %. On the other hand, **PDAT-DTBT-2F** reveals lower contrasts as the extent of oxidative process is hindered. For all three polymers, high coloration efficiencies (CE) were measured at 95 % of the full switch in both the visible and NIR regions, suggesting low power requirements for the operation of such devices. Interestingly, the introduction of fluorine atoms onto the polymers appears to result in higher CE values. Compared to the unfluorinated analogue, enhancements by approximately 15 % to 60 % are observed for **PDAT-DTBT-F** and **PDAT-DTBT-2F** respectively. While the underlying reasons behind such improvements are unclear, it may be due to the more open morphology of the fluorinated polymers as a result of increased surface roughness, which is favorable for lower contact resistance.[46] In addition, better charge transport properties in the fluorinated polymers may have also been possible owing to better polymer packing. Evidence for the morphological differences among the polymers are provided and discussed later (*vide infra*).

As previously mentioned, fluorinated polymers have been found to exhibit better stability in electronic devices such as solar cells and thin-film transistors, possibly attributed to the lower HOMO which reduces the propensity towards atmospheric degradation. In this work, the stabilities of the ECDs were investigated by subjecting the cells to repeated redox cycling between +1.6 and –1.6 V with a residence time of 15 s, while monitoring the changes in optical contrasts. The degradation profiles are shown in Fig. S14. A 'break-in' period of about 80 cycles was observed for all three polymers. Notably of interest is the stark difference in the rate of degradation at the first few cycles. Degradation occurs most rapidly for the unfluorinated polymer, followed by **PDAT-DTBT-F** and lastly, **PDAT-DTBT-2F**. For electrochromic polymers, the redox reversibility is highly dependent on the reactivity/stability of the radical cations (polarons) formed upon electrochemical oxidation. Typically, attack by nucleophiles in close proximity can result in a break in polymer conjugation, leading to irreversible electrochemical doping.[47] In this case, the enhanced stability of fluorinated polymers most likely arose from various pathways, namely, their deeper HOMO levels which inhibit oxidative degradation as well as hydrophobicity of the fluorocarbons which serves to repel neighbouring nucleophiles such as water molecules present in the electrochromic device. After equilibrium, **PDAT-DTBT** shows a 5 % drop in optical contrast after more than 950 cycles for the best trial. On the other hand, both fluorinated **PDAT-DTBT-F** and **PDAT-DTBT-2F** devices reveal excellent ambient stability, revealing no loss in optical contrasts (Fig. 5). Curiously, the optical contrasts increase by approximately 7 and 18 % for **PDAT-DTBT-F** and **PDAT-DTBT-2F** respectively. On the average for 3 repeated trials, the changes in optical contrasts over 950 cycles are 18 % decrease, 5 % decrease and 3 % increase for **PDAT-DTBT**, **PDAT-DTBT-F** and **PDAT-DTBT-2F** respectively, demonstrating the reproducible enhanced stabilities of the fluorinated polymers. Long-

term stability testing was further carried out for **PDAT-DTBT-F**. The device was cycled for 800–1200 cycles per day between +1.6 and –1.6 V at 1500 nm, over the course of approximately 2 weeks. Over the entire duration, the device was stored under ambient conditions without any additional encapsulation. Over 10 000 deep potential steps, insignificant degradation was observed (Fig. 6). More than 90 % of the optical contrast was retained, confirming the high redox stability of the fluorinated polymers.

Thin film morphology

The microstructures of the polymer films were analyzed using XRD measurements (Fig. 7). For all three polymers, distinct (100) reflection was observed, of which the *d*-spacing corresponds to the in-plane spacing of the polymers. Interestingly, the diffraction peak intensities increase, with the peak maxima slightly shifted to larger angles upon the addition of fluorine atoms. As such, the in-plane spacing ($d_{(100)}$) decreases along the trend (Fig. 7). Nevertheless, a more pronounced effect is observed going from **PDAT-DTBT** to **PDAT-DTBT-F**, and less from **PDAT-DTBT-F** to **PDAT-DTBT-2F**. The results suggest that the fluorinated polymers possess better molecular ordering and interaction, which supports the obtained spectroscopic data. The efficient packing and self-organization of the polymer chains may have also contributed to better charge transport and enhanced switching behavior.

The surface morphologies of the polymer films were also probed using atomic force microscopy and the height images are shown in Fig. 8. In all the three polymers, homogeneous and uniform surfaces are observed. In particular, the presence of fibrillar crystalline domains is most apparent in **PDAT-DTBT-2F**. Moreover, it has been revealed that the mean roughness increases slightly with the successive addition of fluorine atoms. This could possibly be attributed to the reduced solubility of the fluorinated polymers, which readily aggregate as the solvent evaporates during the spin-coating process.[43] It has been observed that the film morphology critically affects the electrochromic performance of the polymers.[13, 48] While a rough surface with an open, porous structure[49, 50] has largely been believed to be favorable for rapid switching, the exact mechanism is however not yet fully understood. Further investigations are thus required to correlate the film morphology and polymer crystallinity with the electrochromic performance.

Conclusions

A series of BTD-containing D− A type conjugated polymers was synthesized with two fluorinated analogues (**PDAT-DTBT**, **PDAT-DTBT-F** and **PDAT-DTBT-2F**). The introduction of fluorine atoms onto the polymer backbone was found to have an influence on the optical, electrochemical, and morphological properties of the polymers. In addition, the effect of fluorination was investigated in electrochromic devices. Fluorination of electron acceptors was able to markedly enhance the polymer reduction process to sub-second speeds, as well as improve the coloration efficiencies of the devices. More importantly, in comparison with non-fluorinated counterpart, fluorinated polymers were found to exhibit exceptional electrochemical stability even under ambient conditions and without any additional encapsulation of devices. **PDAT-DTBT-F** device was tested up to 10, 000 deep potential cycles, without noteworthy loss in optical contrast. It is envisaged that fluorination of building blocks of conjugated polymers, in particular electron-deficient acceptors, would offer an alternative promising design strategy towards highly ambient-stable electrochromic polymers.

Experimental

Materials

All chemicals were purchased from Sigma-Aldrich, Alfa Aesar, Derthon Optoelectronic Materials Science Technology Co Ltd or Strem and used as received. Tetrahydrofuran (THF) was distilled over sodium benzophenone ketyl before use. The syntheses of **3a** and **4a** have been reported previously.[42] ITO-coated glass substrates (15 Ω/sq, 35×30×1.1mm) were purchased from Xinyan Technology Ltd.

Monomer synthesis

3,4-Bis(2-hexyldecyloxy)thiophene (1). This compound was synthesized in 99% yield using a method adapted from literature.[40] ^{1}H NMR ($CDCl_3$, 400 MHz) δ 6.15 (s, 2H), 3.84-3.82 (d, 4H, J = 6.0 Hz), 1.80-1.79 (m, 2H), 1.42-1.32 (m, 48H), 0.89–0.86 (t, 12H).

2,5-Dibromo-3,4-bis(2-hexyldecyloxy)thiophene (2). This compound was synthesised in 92% yield using a method adapted from literature.[41] ^{1}H NMR (CD_2Cl_2, 400 MHz) δ 3.97-3.96 (d, 4H, J = 5.6 Hz), 1.72 (m, 2H), 1.49-1.31 (m, 48H), 0.90–0.89 (m, 12H). ^{13}C NMR ($CDCl_3$, 100 MHz) δ 148.3, 95.1, 39.2, 32.3, 31.5, 30.5, 30.1, 30.1, 29.8, 27.3, 23.1, 14.5. Anal. calcd. for $C_{36}H_{66}Br_2O_2S$: C, 59.82; H, 9.20; S, 4.44. Found C, 60.33; H, 9.28; S, 3.42.

5-Fluoro-4,7-bis(thien-2-yl)benzo-2,1,3-thiadiazole (3b). A 20 mL microwave glass vial was charged with a stirring bar, 4,7-dibromo-5-fluorobenzo-2,1,3-thiadiazole (1.59 g, 5 mmol), 2-(tributylstannyl)thiophene (4.66 g, 12.5 mmol) and tetrakis(triphenylphosphine)palladium (0) (115 mg, 2.5 mol%). DMF (15 mL) was added and the vial was then sealed. The vial was then heated at 120 °C for 2 min and then 160 °C for 20 min in a microwave reactor. After cooling, the DMF was removed under reduced pressure. The residue was redissolved in dichloromethane and washed with dilute hydrochloric acid, 1M NaOH and water. The title compound was obtained as orange crystals after recrystallization in ethanol/chloroform. ^{1}H NMR (CD_2Cl_2, 400 MHz) δ 8.31-8.30 (d, 1H, J = 3.6 Hz), 8.18-8.17 (d, 1H, J = 3.6 Hz), 7.87-7.84 (d, 1H, J = 13.2 Hz), 7.62-7.60 (d, 1H, J = 5.2 Hz), 7.57-7.56 (d, 1H, J = 4.8 Hz), 7.28-7.24 (m, 2H).

5,6-Difluoro-4,7-bis(thien-2-yl)benzo-2,1,3-thiadiazole (3c). This compound was synthesized from 4,7-dibromo-5,6-fluorobenzo-2,1,3-thiadiazole as orange crystals in 67.9% yield using a similar procedure as that for **3b**. ^{1}H NMR ($CDCl_3$, 400 MHz) δ 8.31-8.30 (d, 2H, J = 3.6 Hz), 7.63-7.62 (d, 2H, J = 5.2 Hz), 7.29-7.28 (d, 2H, J = 4.4 Hz).

5-fluoro-4,7-bis(5-trimethylstannyl-thien-2-yl)benzo-2,1,3-thiadiazole (4b). This compound was synthesized from **3b** in 53% yield using a method adapted from literature.[42] ^{1}H NMR (CD_2Cl_2, 400 MHz) δ 8.36-8.35 (d, 1H, J = 3.2 Hz), 7.39-7.38 (d, 1H, J = 3.6 Hz), 7.85-7.82 (d, 1H, J = 12.8 Hz), 7.37-7.36 (d, 1H, J = 3.2 Hz), 7.34-7.33 (d, 1H, J = 3.6 Hz), 0.45 (s, 18H). ^{13}C NMR ($CDCl_3$, 100 MHz) δ 160.4, 157.9, 150.3, 144.1, 142.3, 141.7, 138.5, 136.6, 135.7, 131.3, 131.2, 129.6, 117.6, 117.2, -7.6. ^{19}F NMR ($CDCl_3$, 470 MHz) δ -108.4. Anal. calcd. for $C_{20}H_{23}FN_2S_3Sn_2$: C, 37.30; H, 3.60; N, 4.35; S, 14.94. Found C, 37.34; H, 3.46; N, 4.29; S, 14.67.

5,6-difluoro-4,7-bis(5-trimethylstannyl-thien-2-yl)benzo-2,1,3-thiadiazole (4c). This compound was synthesized from **3c** in 67% yield using a method adapted from literature.[42] ^{1}H NMR (CD_2Cl_2, 400 MHz) δ 8.38-8.37 (d, 2H, J = 3.6 Hz), 7.39-7.38 (d, 2H, J = 3.6 Hz), 0.47 (s, 18H). ^{13}C NMR ($CDCl_3$, 100 MHz) δ 151.4, 149.5, 143.0, 137.5, 135.8, 132.0, 112.1, -7.7. ^{19}F NMR ($CDCl_3$, 470 MHz) δ -127.9. Anal. calcd. for $C_{20}H_{22}F_2N_2S_3Sn_2$: C, 36.29; H, 3.35; N, 4.23; S, 14.53. Found C, 36.72; H, 3.25; N, 4.23; S, 14.69.

Polymer synthesis

General procedure for Stille copolymerization. The dibromo and bis-stannylated monomers (1 equivalent each) were added to a reaction vial equipped with a magnetic stirrer. The vial was then transferred to a glovebox where tris-(dibenzylideneacetone)dipalladium(0) (4 mol%), tri(o-tolyl)-phosphine (16 mol%) and anhydrous chlorobenzene (20 mL) were added. The vial was then heated at 120 °C for 72 hours using an oil bath. The reaction mixture was poured into 200 mL of methanol and 10 mL of concentrated hydrochloric acid and stirred overnight to remove the stannylated end-groups. The polymer was filtered and subjected to Soxhlet extraction with methanol (12 h), hexanes (12 h), and chloroform (12 h). The chloroform fraction was then concentrated, precipitated into 200 mL of methanol, filtered and dried to obtain the final product.

PDAT-DTBT. Yield 85%. ^{1}H NMR ($C_2D_2Cl_4$, 400 MHz, 120 °C) δ 8.17 (s, 2H), 7.94 (s, 2H), 7.47 (s, 2H), 4.20 (s, 4H), 2.08 (s, 2H), 1.51-1.39 (m, 48H), 0.95 (s, 12H). Anal. calcd. for $C_{50}H_{72}N_2O_2S_4$: C, 69.72; H, 8.42; N, 3.25; S, 14.89. Found C, 69.44; H, 8.18; N, 3.38; S, 15.38. HT-GPC M_n: 12.9 kg mol^{-1}, M_w: 48.4 kg mol^{-1}, PDI: 3.74.

PDAT-DTBT-F. Yield 71%. ^{1}H NMR ($C_2D_2Cl_4$, 400 MHz, 120 °C) δ 8.32 (s, 1H), 8.18 (s, 1H), 7.82 (s, 1H), 7.48 (s, 2H), 4.22 (s, 4H), 2.11 (s, 2H), 1.52-1.42 (m, 48H), 0.97 (s, 12H). ^{19}F NMR ($C_2D_2Cl_4$, 470 MHz) δ -107.6. Anal. calcd. for $C_{50}H_{71}FN_2O_2S_4$: C, 68.29; H, 8.14; N, 3.19; S, 14.59. Found C, 68.41; H, 7.81; N, 3.40; S, 14.44. HT-GPC M_n: 20.0 kg mol^{-1}, M_w: 55.6 kg mol^{-1}, PDI: 2.78.

PDAT-DTBT-2F. Yield 57%. ^{1}H NMR ($C_2D_2Cl_4$, 400 MHz, 120 °C) δ 8.34 (s, 2H), 7.68 (s, 2H), 4.22 (s, 4H), 2.12 (s, 2H), 1.69-1.42 (m, 48H), 0.96 (s, 12H). ^{19}F NMR ($C_2D_2Cl_4$, 470 MHz) δ -127.7. Anal. calcd. for $C_{50}H_{69}F_2N_2O_2S_4$: C, 66.92; H, 7.86; N, 3.12; S, 14.29. Found C, 65.73; H, 7.30; N, 3.48; S, 14.08. HT-GPC M_n: 6.7 kg mol^{-1}, M_w: 12.6 kg mol^{-1}, PDI: 1.88.

Electrochromic device fabrication

ITO/glass substrates were cleaned by successive ultrasonication in acetone, isopropyl alcohol and distilled water, and blown dry with N_2 prior to use. Polymer solutions of **PDAT-DTBT**, **PDAT-DTBT-F** and **PDAT-DTBT-2F** (8 mg/mL in 1:3 (v/v) chloroform:chlorobenzene) were filtered and spin-coated onto the ITO substrates at 600 rpm for 60 s to yield film thickness of around 30 nm. Excessive polymer edges were removed by swabbing with chloroform using a cotton bud to obtain an active area of 2×2 cm^2. On a second piece of ITO substrate, an area of 2×2 cm^2 was blocked out using parafilm. The total thickness of the parafilm spacer and barrier was kept constant at 0.01". 250 μL of the gel electrolyte (0.512 g of lithium perchlorate and 2.8 g of poly(methyl methacrylate) (MW = 120 000 g/mol) in 6.65 ml of propylene carbonate and 28 ml of dry acetonitrile (ACN) was pipetted within the 2×2 cm^2 area and left to dry for 5 minutes. The device was fabricated by assembling the two ITO/glass substrates together with the polymer film and gel electrolyte in contact.

Instrumentation

^{1}H and ^{13}C NMR were performed using a Bruker Avance 400 spectrometer. 19F NMR was performed using a JEOL ECA500II spectrometer. TGA was performed using a TGA Q500 from TA Instruments. DSC was performed using a PDSC Q100 from TA instruments. Gel permeation chromatography was carried out at 160 ° C using an Agilent PL 220 system using a refractive index detector and 1,2,4-trichlorobenzene as the eluent. All UV-vis/UV-vis-NIR absorption spectra were recorded using a Shimadzu UV-3600 UV-vis-NIR spectrophotometer. Cyclic voltammetry experiments were carried out using an Autolab PGSTAT128N potentiostat. Measurements were done in a MBraun LABmaster 130 glove box, in a three-electrode cell configuration with polymer-coated glassy carbon, Pt wire and Ag wire as the working, counter and pseudo-reference electrodes respectively. A 0.1 M LiClO4/ACN electrolyte/solvent couple was used and all measurements were recorded at 50 mV/s. The pseudo-reference electrode was calibrated against the ferrocene/ferrocenium redox couple. All electrochromic studies were performed in-situ, using both the potentiostat and spectrophotometer. AFM images were obtained under tapping mode, using a Bruker Dimension Icon^{TM} atomic force microscope. X-ray diffraction (XRD) patterns of the thin films were recorded in reflection mode with a Cu-Kα radiation source (λ = 0.15406 nm) on a Bruker D8 General Area Detector Diffraction System.

Acknowledgements

This research was supported by Agency for Science, Technology and Research (A*STAR) and Ministry of National Development (MND) Green Building Joint Grant (No. 1321760011). This work was supported by the A*STAR Computational Resource Centre through the use of its high performance computing facilities. We would like to thank Mr. Lim Poh Chong for the XRD measurements, and Mr. Goh Tai Wei, Glen for the AFM images.

Notes and references

[a] Institute of Materials Research and Engineering, Agency for Science, Technology and Research (A*STAR), 3 Research Link, Singapore 117602

[b] NUS Graduate School for Integrative Sciences and Engineering, National University of Singapore, 28 Medical Drive, Singapore 117456

[c] Department of Electrical and Computer Engineering, National University of Singapore, 4 Engineering Drive 3, Singapore 117583

[d] Department of Chemistry, National University of Singapore, 3 Science Drive 3, Singapore 117543

[†] These authors contributed equally to this manuscript.

Electronic Supplementary Information (ESI) available: NMR, TGA, DSC and GPC plots, degradation profile of electrochromic devices, TD-DFT calculations.

1. C. M. Amb, A. L. Dyer and J. R. Reynolds, *Chem. Mater.*, 2010, **23**, 397-415.
2. C.-J. Chen, H.-J. Yen, Y.-C. Hu and G.-S. Liou, *J. Mater. Chem. C*, 2013, **1**, 7623-7634.
3. G. E. Gunbas, A. Durmus and L. Toppare, *Adv. Funct. Mater.*, 2008, **18**, 2026-2030.
4. J. Jensen, M. Hösel, I. Kim, J.-S. Yu, J. Jo and F. C. Krebs, *Adv. Funct. Mater.*, 2014, **24**, 1228-1233.
5. J. A. Kerszulis, K. E. Johnson, M. Kuepfert, D. Khoshabo, A. L. Dyer and J. R. Reynolds, *J. Mater. Chem. C*, 2015, DOI: 10.1039/C4TC02685C.
6. J. A. Kerszulis, C. M. Amb, A. L. Dyer and J. R. Reynolds, *Macromolecules*, 2014, **47**, 5462-5469.
7. J. Kim, J. You, B. Kim, T. Park and E. Kim, *Adv. Mater.*, 2011, **23**, 4168-4173.
8. B. Weng, S. Ashraf, P. C. Innis and G. G. Wallace, *J. Mater. Chem. C*, 2013, **1**, 7430-7439.
9. H.-J. Yen, H.-Y. Lin and G.-S. Liou, *Chem. Mater.*, 2011, **23**, 1874-1882.
10. V. K. Thakur, G. Ding, J. Ma, P. S. Lee and X. Lu, *Adv. Mater.*, 2012, **24**, 4071-4096.
11. M. Icli-Ozkut, H. Ipek, B. Karabay, A. Cihaner and A. M. Onal, *Polym. Chem.*, 2013, **4**, 2457-2463.
12. Q. Ye, W. T. Neo, C. M. Cho, S. W. Yang, T. Lin, H. Zhou, H. Yan, X. Lu, C. Chi and J. Xu, *Org. Lett.*, 2014, **16**, 6386-6389.
13. Q. Ye, W. T. Neo, T. Lin, J. Song, H. Yan, H. Zhou, K. W. Shah, S. J. Chua and J. Xu, *Polym. Chem.*, 2015, **6**. 1487-1494.
14. C. M. Amb, P. M. Beaujuge and J. R. Reynolds, *Adv. Mater.*, 2010, **22**, 724-728.
15. P. M. Beaujuge, S. Ellinger and J. R. Reynolds, *Adv. Mater.*, 2008, **20**, 2772-2776.
16. P. M. Beaujuge, S. V. Vasilyeva, S. Ellinger, T. D. McCarley and J. R. Reynolds, *Macromolecules*, 2009, **42**, 3694-3706.
17. P. M. Beaujuge, S. V. Vasilyeva, D. Y. Liu, S. Ellinger, T. D. McCarley and J. R. Reynolds, *Chem. Mater.*, 2012, **24**, 255-268.
18. Ö. Çelikbilek, M. İçli-Özkut, F. Algi, A. M. Önal and A. Cihaner, *Org. Electron.*, 2012, **13**, 206-213.
19. M. İçli, M. Pamuk, F. Algi, A. M. Önal and A. Cihaner, *Chem. Mater.*, 2010, **22**, 4034-4044.
20. M. Karakus, A. Balan, D. Baran, L. Toppare and A. Cirpan, *Synth. Met.*, 2012, **162**, 79-84.
21. M. Sendur, A. Balan, D. Baran, B. Karabay and L. Toppare, *Org. Electron.*, 2010, **11**, 1877-1885.
22. P. Shi, C. M. Amb, A. L. Dyer and J. R. Reynolds, *ACS Appl. Mater. Interfaces*, 2012, **4**, 6512-6521.
23. P. Shi, C. M. Amb, E. P. Knott, E. J. Thompson, D. Y. Liu, J. Mei, A. L. Dyer and J. R. Reynolds, *Adv. Mater.*, 2010, **22**, 4949-4953.
24. S. V. Vasilyeva, P. M. Beaujuge, S. Wang, J. E. Babiarz, V. W. Ballarotto and J. R. Reynolds, *ACS Appl. Mater. Interfaces*, 2011, **3**, 1022-1032.
25. A. Iyer, J. Bjorgaard, T. Anderson and M. E. Köse, *Macromolecules*, 2012, **45**, 6380-6389.
26. J. W. Jo, S. Bae, F. Liu, T. P. Russell and W. H. Jo, *Adv. Funct. Mater.*, 2015, **1**, 120-125.
27. J. Kim, M. H. Yun, G.-H. Kim, J. Lee, S. M. Lee, S.-J. Ko, Y. Kim, G. K. Dutta, M. Moon, S. Y. Park, D. S. Kim, J. Y. Kim and C. Yang, *ACS Appl. Mater. Interfaces*, 2014, **6**, 7523-7534.
28. J.-H. Kim, S. A. Shin, J. B. Park, C. E. Song, W. S. Shin, H. Yang, Y. Li and D.-H. Hwang, *Macromolecules*, 2014, **47**, 1613-1622.
29. Y. Lu, Z. Xiao, Y. Yuan, H. Wu, Z. An, Y. Hou, C. Gao and J. Huang, *J. Mater. Chem. C*, 2013, **1**, 630-637.
30. B. C. Schroeder, Z. Huang, R. S. Ashraf, J. Smith, P. D'Angelo, S. E. Watkins, T. D. Anthopoulos, J. R. Durrant and I. McCulloch, *Adv. Funct. Mater.*, 2012, **22**, 1663-1670.
31. P. Shen, H. Bin, Y. Zhang and Y. Li, *Polym. Chem.*, 2014, **5**, 567-577.
32. T. Umeyama, Y. Watanabe, E. Douvogianni and H. Imahori, *J. Phys. Chem. C*, 2013, **117**, 21148-21157.
33. N. Wang, Z. Chen, W. Wei and Z. Jiang, *J. Am. Chem. Soc.*, 2013, **135**, 17060-17068.
34. X. Wang, Z.-G. Zhang, H. Luo, S. Chen, S. Yu, H. Wang, X. Li, G. Yu and Y. Li, *Polym. Chem.*, 2014, **5**, 502-511.
35. Y. Yang, R. Wu, X. Wang, X. Xu, Z. Li, K. Li and Q. Peng, *Chem. Comm.*, 2014, **50**, 439-441.
36. Y. Zhang, S.-C. Chien, K.-S. Chen, H.-L. Yip, Y. Sun, J. A. Davies, F.-C. Chen and A. K. Y. Jen, *Chem. Comm.*, 2011, **47**, 11026-11028.
37. H. Zhou, L. Yang, A. C. Stuart, S. C. Price, S. Liu and W. You, *Angew. Chem. Int. Ed.*, 2011, **50**, 2995-2998.
38. T. Lei, J.-H. Dou, Z.-J. Ma, C.-H. Yao, C.-J. Liu, J.-Y. Wang and J. Pei, *J. Am. Chem. Soc.*, 2012, **134**, 20025-20028.
39. U. Giovanella, C. Botta, F. Galeotti, B. Vercelli, S. Battiato and M. Pasini, *J. Mater. Chem. C*, 2013, **1**, 5322-5329.

40. S. Jiang, P. Shen, P. Jiang, W. Zhou, B. Zhao, Y. Liu and S. Tan, *Eur. Polym. J.*, 2011, **47**, 2424-2431.
41. W. Zhang, F. Tao, L.-y. Xi, K.-g. Meng, Z. Wang, Y. Li and Q. Jiang, *J Mater Sci*, 2012, **47**, 323-331.
42. K. H. Ong, S. L. Lim, H. S. Tan, H. K. Wong, J. Li, Z. Ma, L. C. H. Moh, S. H. Lim, J. C. de Mello and Z. K. Chen, *Adv. Mater.*, 2011, **23**, 1409-1413.
43. H. Bronstein, J. M. Frost, A. Hadipour, Y. Kim, C. B. Nielsen, R. S. Ashraf, B. P. Rand, S. Watkins and I. McCulloch, *Chem. Mater.*, 2013, **25**, 277-285.
44. A. K. Agrawal and S. A. Jenekhe, *Chem. Mater.*, 1996, **8**, 579-589.
45. T. Taerum, O. Lukoyanova, R. G. Wylie and D. F. Perepichka, *Org. Lett.*, 2009, **11**, 3230-3233.
46. C.-G. Wu, M.-I. Lu and M.-F. Jhong, *J. Polym. Sci Part B: Polym. Phys.*, 2008, **46**, 1121-1130.
47. A. A. Pud, *Synth. Met.*, 1994, **66**, 1-18.
48. W. T. Neo, Q. Ye, T. T. Lin, S. J. Chua and J. Xu, *Sol. Energy Mater. Sol. Cells*, 2015, **136**, 92-99.
49. J.-H. Huang, C.-Y. Hsu, C.-W. Hu, C.-W. Chu and K.-C. Ho, *ACS Appl. Mater. Interfaces*, 2010, **2**, 351-359.
50. P. Tehrani, L.-O. Hennerdal, A. L. Dyer, J. R. Reynolds and M. Berggren, *J. Mater. Chem.*, 2009, **19**, 1799-1802.

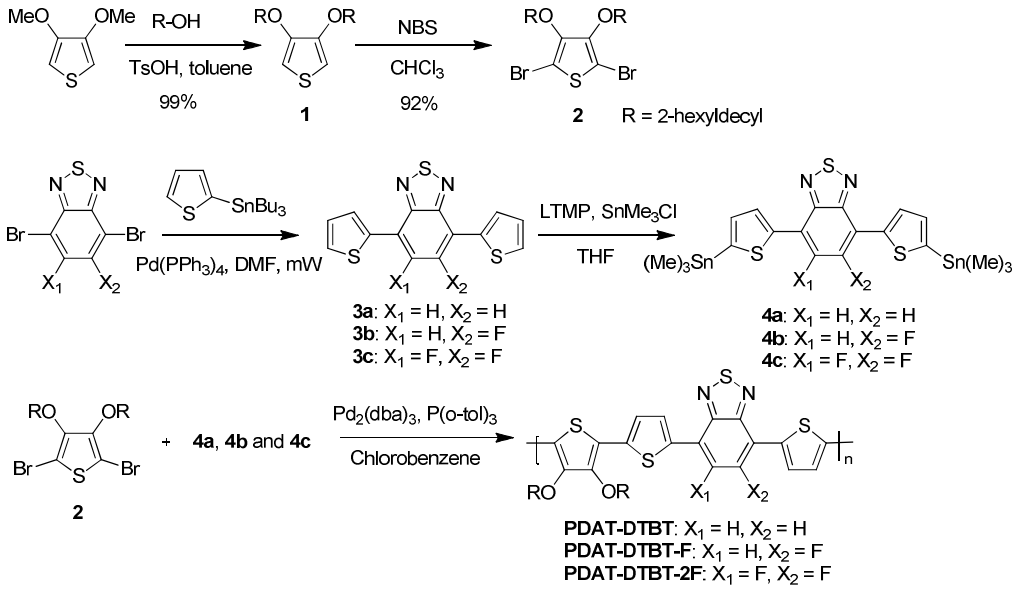

Scheme 1 Synthetic routes of monomers and polymers for **PDAT-DTBT** polymers.

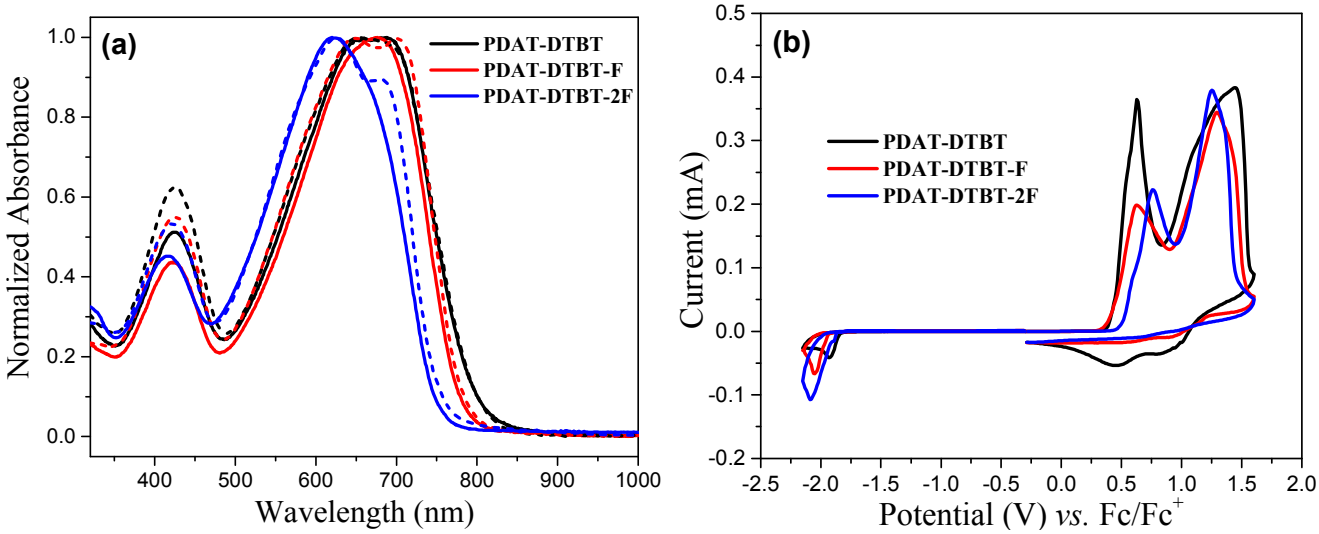

Fig. 1 (a) Normalized UV-vis absorption spectra of polymers in chlorobenzene (solid lines) and as thin films (dashed lines). (b) Cyclic voltammograms of polymer thin films in 0.1M $LiClO_4$/acetonitrile (ACN) electrolyte/solvent couple at a scan rate of 50 mV/s calibrated vs. ferrocene/ferrocenium couple.

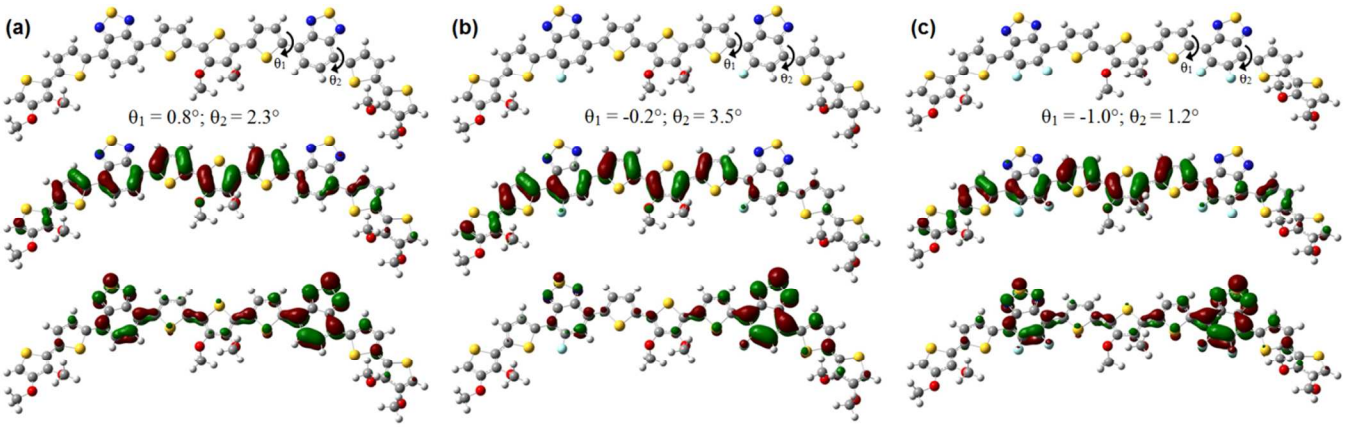

Fig. 2 Optimized geometries (top) and charge-density isosurfaces for the HOMO (middle) and LUMO (bottom) levels of (a) **PDAT-DTBT**, (b) **PDAT-DTBT-F** and (c) **PDAT-DTBT-2F** dimers (B3LYP/6-31G).

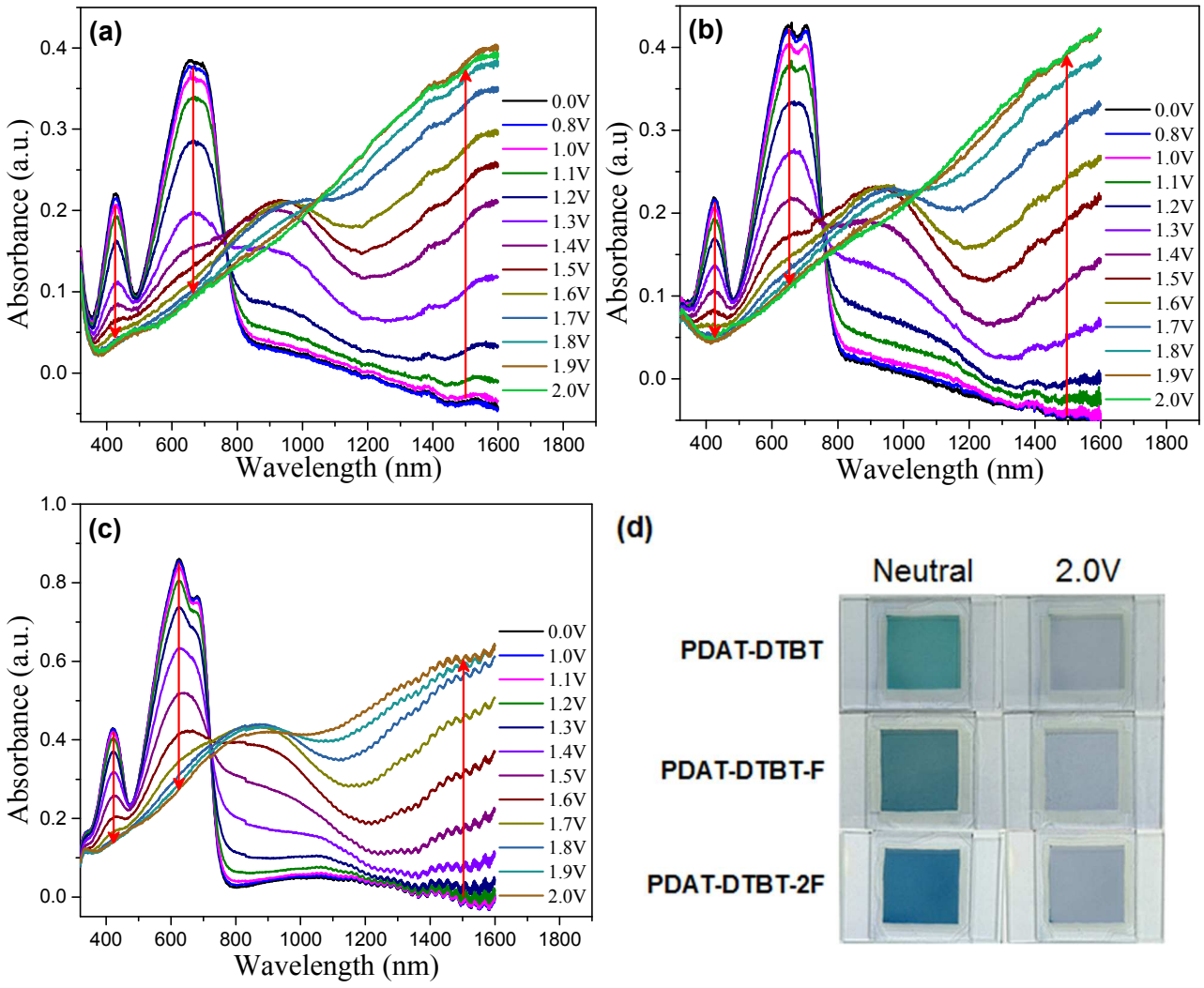

Fig. 3 Spectroelectrochemical graphs of (a) **PDAT-DTBT**, (b) **PDAT-DTBT-F** and (c) **PDAT-DTBT-2F** devices at various applied potentials. (d) Colors of the devices in their neutral and 2.0 V states.

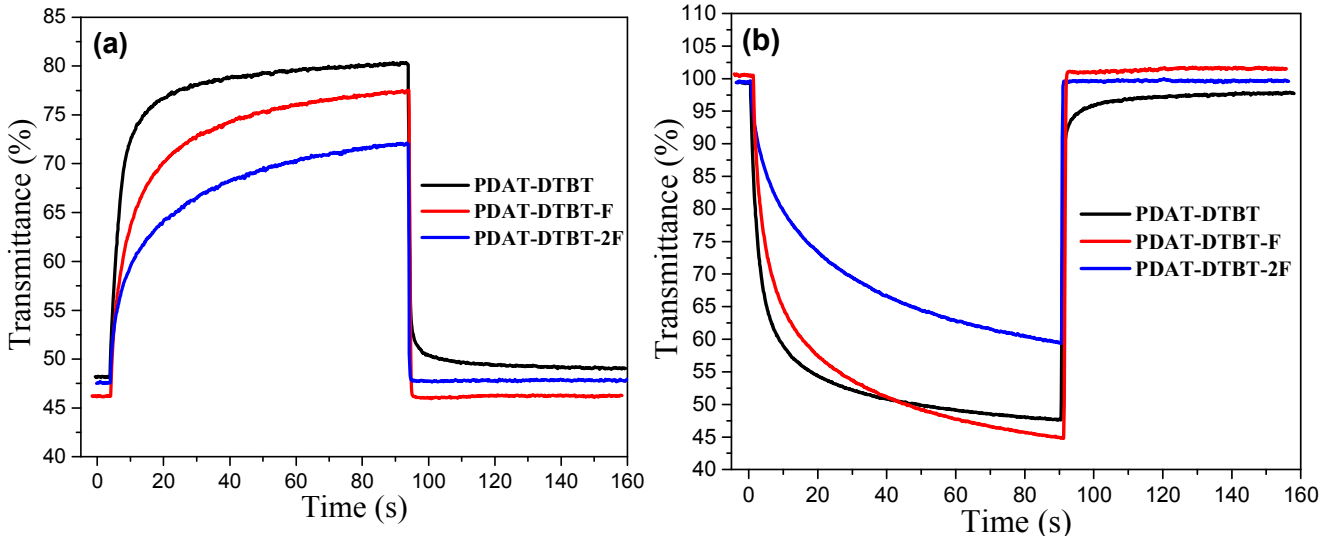

Fig. 4 Switching cycles of **PDAT-DTBT**, **PDAT-DTBT-F** and **PDAT-DTBT-2F** devices in the (a) visible (λ_{max}) and (b) NIR (1500 nm) regions between + 1.6 and -1.6 V.

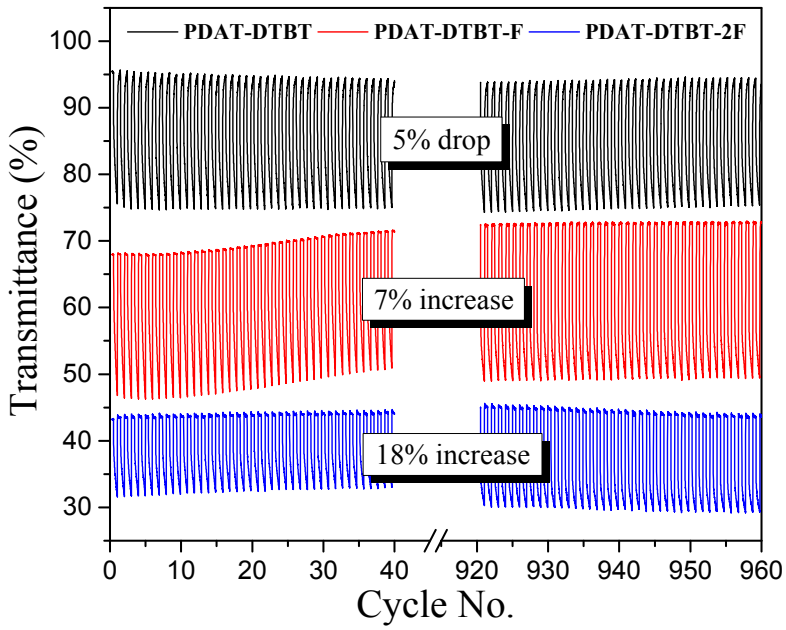

Fig. 5 Long term ambient stability of **PDAT-DTBT**, **PDAT-DTBT-F** and **PDAT-DTBT-2F** devices switched at 15 s cycles between + 1.6 and -1.6 V at 1500 nm. The graphs are offset for clarity and do not reflect the actual transmittance values.

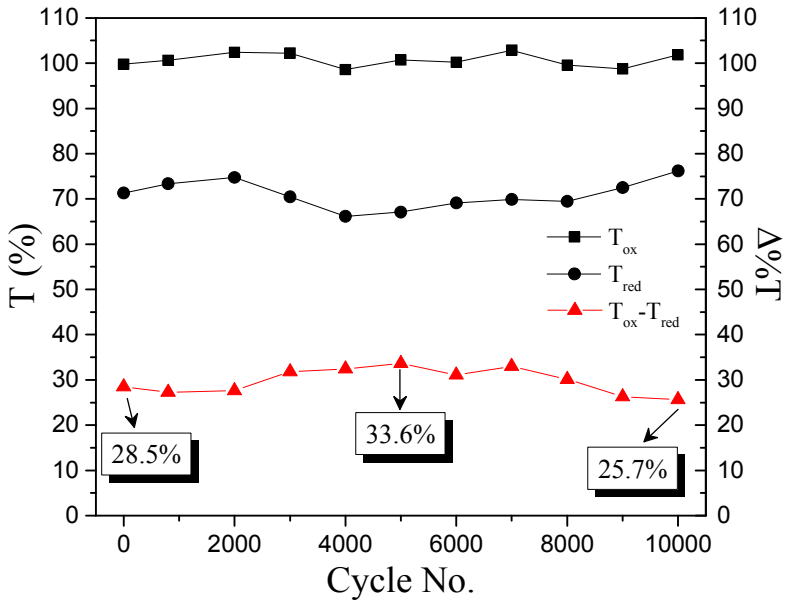

Fig. 6 Long-term ambient stability testing of **PDAT-DTBT-F** electrochromic device switched at 15 s cycles between +1.6 and -1.6 V at 1500 nm.

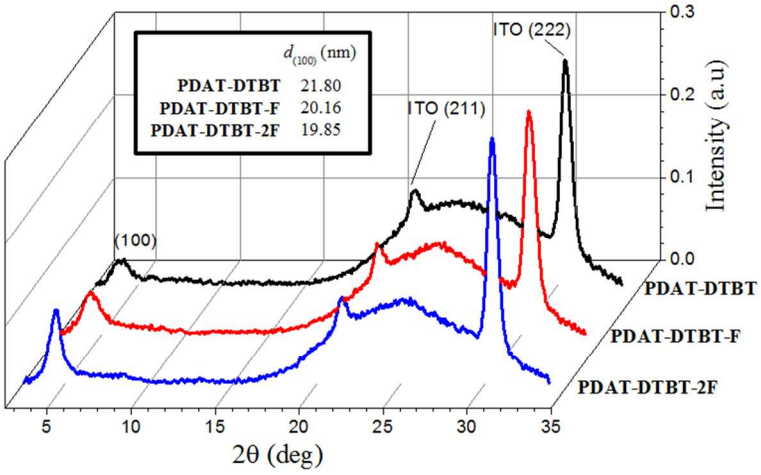

Fig. 7 XRD spectra of **PDAT-DTBT**, **PDAT-DTBT-F** and **PDAT-DTBT-2F** thin films drop cast on ITO/glass substrates.

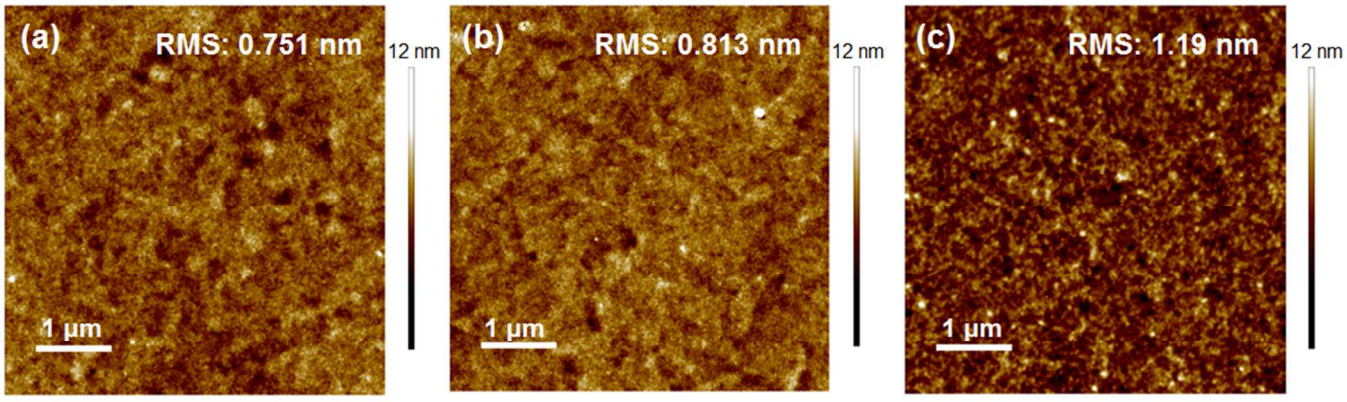

Fig. 8 AFM images of (a) **PDAT-DTBT**, (b) **PDAT-DTBT-F** and (c) **PDAT-DTBT-2F** spin-coated thin films. The scan size of the images is 5 × 5 μm.

Table 1 Synthetic Yields, Molecular Weights, Polydispersity and Thermal Data of Polymers

Polymer	Yield (%)	M_n (kg mol^{-1})	M_w (kg mol^{-1})	Polydispersity	T_d (in N_2)
PDAT-DTBT	85	12.9	48.4	3.74	335
PDAT-DTBT-F	71	20.0	55.6	2.78	335
PDAT-DTBT-2F	57	6.7	12.6	1.88	335

M_n: the number-average molecular weight. M_w: the weight-average molecular weight. T_d: the decomposition temperature at which 5% weight loss occurs.

Table 2 Summary of Optical and Electrochemical Properties of Polymers

Polymer	λ_{max} (nm)		λ_{onset} (nm)		E_g^{opt} (eV)[a]	HOMO (eV)[b]	LUMO (eV)[c]
	Solution	Film	Solution	Film			
PDAT-DTBT	424, 652, 690	426, 652, 691	795	800	1.55	-5.22	-3.67
PDAT-DTBT-F	422, 675	424, 648, 702	778	782	1.59	-5.24	-3.65
PDAT-DTBT-2F	416, 622	421, 625, 680	749	772	1.61	-5.31	-3.70

[a] $E_g^{opt} = 1240/\lambda_{onset,film}$. [b] $E_{HOMO} = -(E_{onset,ox\ vs\ ferrocene}) - 4.8$. [c] $E_{LUMO} = E_{HOMO} + E_g^{opt}$.

Table 3 Summary of Electrochromic Performance of ECDs

Polymer	Visible (λ_{max})				NIR (1500 nm)			
	Contrast (%)	τ_b[a] (s)	τ_c[b] (s)	CE[c] (cm^2/C)	Contrast (%)	τ_b[a] (s)	τ_c[b] (s)	CE[c] (cm^2/C)
PDAT-DTBT	31±1	32.7±1.9	4.62±0.46	330±14	52±1	5.90±1.40	41.6±3.3	462±26
PDAT-DTBT-F	31±1	53.2±2.6	0.75±0.03	406±21	56±2	0.70±0.05	57.0±2.2	523±58
PDAT-DTBT-2F	25±1	62.4±1.0	0.42±0.06	524±22	40±2	0.49±0.08	69.3±1.2	748±68

Results are obtained based on 3 trials.
[a] τ_b: bleaching time. Bleaching refers to the process in which the percent transmittance changes from a lower value to a higher value.
[b] τ_c: coloration time. Coloration refers to the process in which the percent transmittance changes from a higher value to a lower value.
[c] Coloration Efficiency

Graphical Abstract

Effects of Fluorination on the Electrochromic Performance of Benzothiadiazole-Based Donor-Acceptor Copolymers

Wei Teng Neo, Kok Haw Ong, Ting Ting Lin, Soo-Jin Chua, and Jianwei Xu*

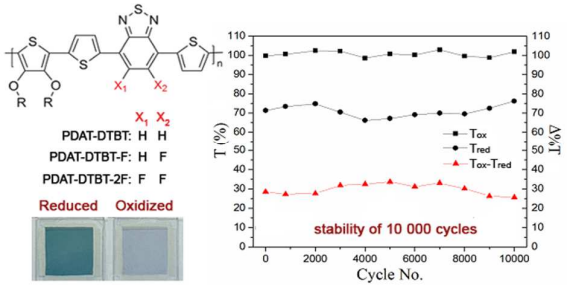

Fluorination of electron acceptors in donor-acceptor type conjugated polymers leads to substantial enhancement in long-term redox stability of electrochromic devices.